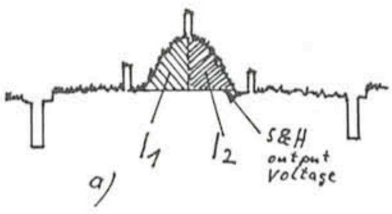

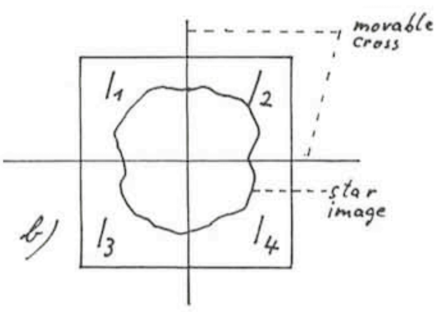

Figure 6a and b.

four integrated values. The address decoding is done on the interface board. When the computer has read the last address all the registers are cleared and a new integration starts automatically.

In the computer the position error is calculated and normalized by:

$$E_x = \frac{I_1 + I_3 - I_2 = I_4}{I_1 + I_2 + I_3 + I_4}$$

$$E_y = \frac{I_1 + I_2 - I_3 - I_4}{I_1 + I_2 + I_3 + I_4}$$

(See Fig. 6b)

The normalization makes the error independent on star magnitudes, seeing effects and HV adjustments of the TV cameras. To keep the servos of the main drive axis of the telescope stable, an additional measure is to avoid an error proportional speed correction. If an error is detected the corrections will be done by constant offset steps in the right direction.

If the normalized error is bigger than 0.15 then an offset step of 0.1 second of arc is applied. If the error is bigger than 0.85 the offset step will be 0.5 second of arc, but this value can be adjusted depending on optical scales and seeing conditions. For an optical scale of 2.5 lines per second of arc the appropriate step size would be 0.″3. If the error is smaller than 0.15 no correction will be applied.

ESO Infrared Specklegraph

C. PERRIER, Observatoire de Lyon, France

Introduction

An infrared specklegraph is available for Visiting Astronomers for use at the 3.6-m telescope F/35 focus. It has briefly been described in the Announcement for Applications in periods 36 to 38. First tested in September 1984, it has since then achieved the expected performances during several runs. However, its theoretical limits have actually been reached only after a dome air-cooling system has been put into operation early this year. In this article we introduce the instrument assuming that the reader already has some knowledge of the short-exposure imaging principles.

The system is based on the slit-scanning technique which allows to obtain one-dimensional images, that is profiles of a source projected onto the scanning direction axis. It aims first of all to diffraction-limited observations; therefore, it is designed for a data rate fast enough to acquire images under conditions of quasi-frozen seeing, and for a spatial sampling adapted to the near-infrared range. The data are stored in the form of individual scans and the data reduction basically yields coadded scans and 1-D visibilities, i. e. Fourier transforms of the source intensity distribution. These visibilities can then be used either directly for size measurements using assumed intensity distribution models or as input to image restoration algorithms.

Instrument Concept

A dedicated dewar equipped with a set of slits and an electronic chain providing a good frequency response is mounted at the F/35 focus on the infrared photometer adaptor (for a description see Moorwood and van Dijsseldonk, *The Messenger,* No. 39, p. 1). The secondary mirror is used to sweep the beam onto the slit and for that purpose is driven with a saw-tooth waveform. During each sweep equally-spaced measures of the flux integrated along the slit are acquired, forming a 1-D image or scan. Rotating the photometer and secondary mirror adaptors gives access to any given position angle (PA).

The requirements have led to an instrument that is a good compromise between good sensitivity in a wide electric bandpass and the specific constraints imposed by the standard infrared instrumental framework. Its current characteristics are shown in Table 1. The system has been optimized for use at L and contains slits adapted to the telescope cut-off frequencies at K, L and M, plus a wide one for medium-resolution imaging. The maximum data rate well matches the less good conditions under which it is still feasible to obtain high-resolution data down to 2 μm: atmospheric correlation time ≥ 20 ms and seeing at V ≤ 3 arcsec. Conversely, the scan time and amplitude may be continuously adjusted up to values sufficiently large to benefit from excellent conditions occurring when the seeing varies slowly. The full resolution of the 3.6-m telescope cannot be achieved at J and H because the usual observing conditions would be too demanding in terms of frequency response; however, it is of course feasible to observe at these wavelengths with the resolution for K.

Part of the acquisition chain is common to both speckle and photometric set-up; this insures some useful standardization. On the contrary, they do not

TABLE 1: SPECKLEGRAPH CHARACTERISTICS

Filters:	wide-band:	J H K L A M
	CVF:	2.43–4.48 μm; 4.26–5.32 μm; resol. ~1/70
Apertures:	diaphragm ∅:	1.5 4.0 10. arcsec. (saturate at M)
	slit width:	0.105 0.159 0.221 arcsec. (5 arcsec. high)
		0.156 0.246 0.464 arcsec. (10 arcsec. high)
Optics:		F/35; linear beam
Detector:	type:	Cincinnati hybrid InSb; – GΩ feedback
	frequency response:	0.8 @ 100 Hz; 0.4 @ 500 Hz
Electronics:	input range:	± 2.5 V after ± 9 V offset & ×1–1024 amplification
	dynamics:	4096 ADC units
Scanning:	wave-form:	saw-tooth linearity < 1 % in useful part
	amplitude:	0–40 arcsec. (for 128 pts)
Sampling:		128 or 256 pts/scan; half for source; half for sky
		20–600 ms/scan (for 128 pts)
Cryogenics:	outer can:	liquid N2; 6–12 h hold time
	inner can:	solid N2 (55–60 K); > 1–2 weeks hold time

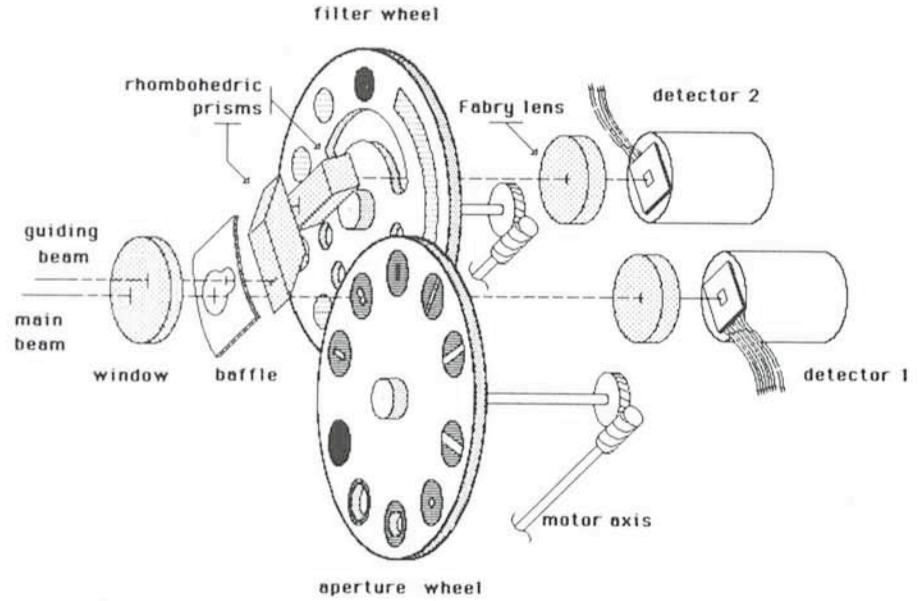

Figure 1: *Schematic of the cold optics.*

share any of the control software nor of the acquisition procedures. In speckle, the secondary mirror control itself is actually part of the acquisition software rather than of the distinct F/35 programme known to infrared observers. The data tape formats also differ largely. So, while the specklegraph might be thought of as a mere additional dewar to be used within the infrared photometric frame, it would not be practicable to change from one set-up to the other during the night.

Optical and Mechanical Design

The cooled optics schematic is given in Figure 1. The very small throughput of the dewar, when used with a slit, has made it possible to choose a linear optical path without pupil reimaging on the filter. This yields a very good beam profile, quite useful for extended sources scanned with a long slit so that very little loss can be expected from this optical arrangement. The use of a Fabry lens has the drawback of chromatism: the optimum adjustment has been done at L which is the best compromise between infrared speckle advantage and degrading sky noise when the wavelength increases.

Figure 1 indeed shows two beams; only the main one is referred to in Table 1. The second one, 8 arcsec off-axis, was initially intended for guiding and seeing monitoring and is equipped with a Santa Babara InSb mounted with a 1 GΩ feedback, a 0.8×5 arcsec^2 slit and an L filter. But the second digitization chain is currently not implemented. Although it can in principle still serve in an analogic way for guiding, practice has proven that this is of little interest as the main beam itself does it more conveniently until the limiting magnitude, depending on seeing conditions, is reached. In fact, this turns out to be more accurate, in the scan direction, than using a guide-star acquired off-axis with the infrared adaptor TV acquisition system. Guiding remains a manual task as scanning prevents the use of the auto-guiding system.

It must be realized that the slits have a fixed orientation (horizontal for a vertical dewar position) whatever the scanning direction on the sky is. As scanning must obviously be perpendicular to them, both adaptors (Cassegrain and secondary mirror) have to be rotated at each new PA setting. While this is straightforward for the latter, it is more time-consuming and requires much caution for the former. The change of PA is thus better restricted to a minimum during the night.

Operation

All instrument functions, that is those of the specklegraph and of the secondary mirror adaptor, are remote-controlled from the User consoles much as in photometry. The software also includes on-line data reduction facilities yielding individual or averaged scans, averaged power spectra and preliminary visibilities and follows the ESO interfacing rules with commands entered either by typing or function keys. The status of the instrument is displayed and updated during acquisition. The DC signal from the detector appears on an oscilloscope which displays every instantaneous image; this is of great help for adjusting the offset and amplification parameters,

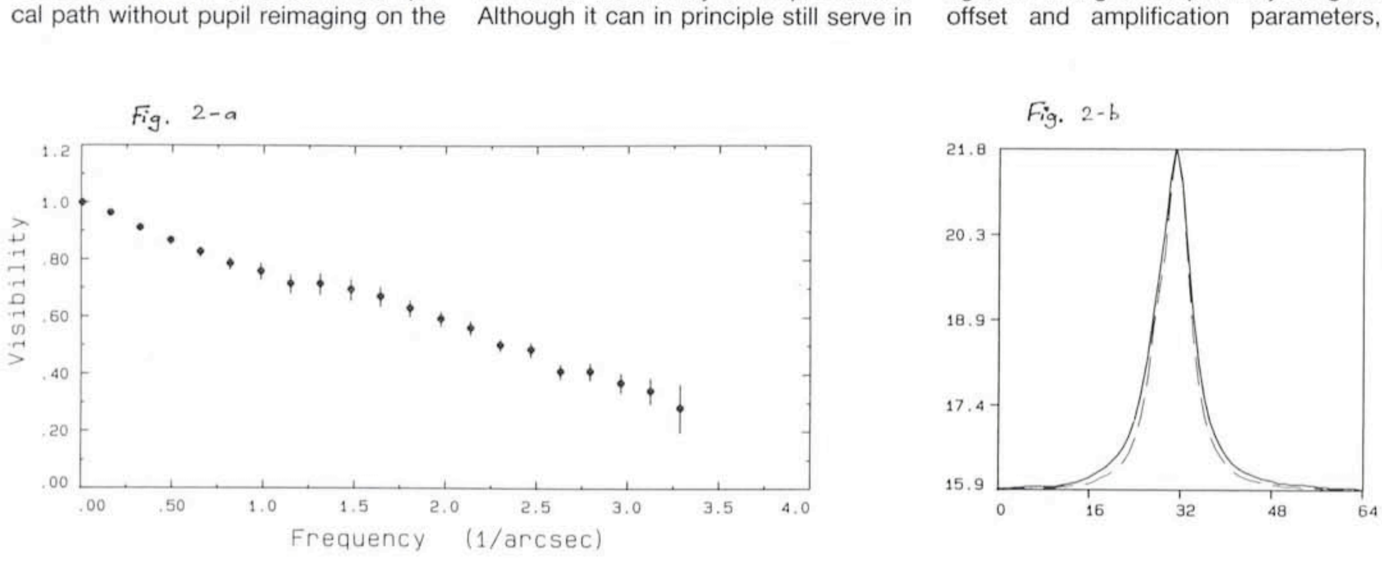

Figure 2: *(a) Visibility at L of an "extended" source. Magnitude at L: 3.5. Exposure time per scan: 100 ms. 1,600 scans retained out of a 16-mn total observing time (reference included). A fit with a 2 gaussian components model gives a diameter of 0.18 ± 0.01 arcsec for the core, contributing 84 ± 3% of the total flux, and 1.5 ± 0.3 arcsec for the halo.*
(b) Coadded recentred scans from the same set of data as in (a). Seeing at V: 1.6 arcsec; full scale: 6.0 arcsec. The dashed curve results from the same treatment applied to the reference star. This graph illustrates the potential access to true imaging by deconvolution techniques using these profiles.

TABLE 2: SPECKLEGRAPH PERFORMANCE

Band:	K	L	M	CVF (3.6 μm)	CVF (4.6 μm)
Limitation source:	system	backgr.	backgr.	system	backgr.
Maxi. spatial frequency (*):	7.9	4.8	3.7	≈4.8	≈3.7
Rayleigh resolution ('):	0.13	0.21	0.27	≈0.21	≈0.27
Saturation with diaphragm:	0.2	−0.4	−1.7	−3.6	−4.2
HIGH RESOLUTION (*) Limiting magnitudes m_o:	7.7	7.0	5.8	4.6	4.5
MEDIUM RESOLUTION (•) Limiting magnitudes m_o:	13.6	11.3	9.3	8.9	8.1

(*) in $arcsec^{-1}$.
(') in arcsec; it gives the size of a source which would be completely resolved; practical resolutions may be 2 or 3 times better depending on the S/N.
(*) Visibility S/N at half resolution: 10, T_t: 15 mn, T_e: 100 ms, W: 1.0 arcsec, $s \approx 1/f_c$. $S/B \approx W^x T_e^y T_t^y s^z$ with $x = -4$, $y = 1/2$, $z = 2$ (sys. lim.), 1 (back. lim.).
(•) Averaged image S/N per seeing element: 3, T_t: 15 mn, T_e: 500 ms, W: 1.0 arcsec, s: 0.46 arcsec, $x = -1/2$, $y = 1/2$, $z = 1/2$ (sys. lim.), 0 (back. lim.).

monitoring the background level and, as mentioned before, fine guiding, but also provides a quick estimation of the atmospheric correlation time t.

Two principles guide the observing procedure: each scan on the source is followed by a scan of equal length on the sky for later sky noise compensation (the scan is thus more than twice the quoted exposure amplitude) and any set of scans on the programme source must be connected to another set on a point-like star (the reference) – obviously with strictly identical settings – in order to correct for the mean atmospheric and optical transfer functions.

One must distinguish between three stages in the course of the observations: the amplitude calibration, usually done once a night on double stars with accurate astrometry (there are not so many); the frequent instrumental parameters setting, specific to each source and including focusing and exposure time adjustement to t.; the acquisition itself, one measurement typically lasting 15 to 30 minutes. Two acquisition modes are available: a static mode where the programme object and its reference star are observed separately, that is by two sequential measurements; a source-switching mode which alternates both sources several times within a unique measurement by offsetting the telescope automatically. This latter procedure, with a switch every 2 to 3 minutes quite specific to speckle interferometry, must always be preferred, the former one being restricted to calibrations or special needs. Because it involves so many parameter settings, it usually seems rather complicated to initiate; however, this is the *only way* to override the seeing variations which decide on the final signal-to-noise ratio, at least for not too faint sources. Its efficiency is optimum for close pairs (< 1°) where the differential pointing, performing extremely well (recentring within half an arcsec happens to be unnecessary after switching!), provides a large gain in total observing time over the static mode in addition to an invaluable qualitative gain. The separation of 1° has been found to be the practical limit beyond which differential seeing effects and optical transfer function variations may not be corrected for.

The basic observing procedure just described does not rule out the need to optimize the operation setting for specified purposes; these go from maximum resolution scanning, which requires a standard speckle setting with fast scans and a slit adapted to the telescope cut-off, to medium resolution imaging and/or close stars photometry, which is better done with slow scans, large amplitude and large slits. These two examples are grossly related, respectively, to the study of very compact sources of magnitudes well below the limiting ones and of somewhat extended, possibly multiple, sources of magnitudes reaching the limits. The software is designed for a large range of parameters and permits such opposite settings, but this flexibility will also not prevent a wrong choice like too long an exposure time under fast seeing or too wide a slit for the desired resolution!

Performances

High spatial resolution imaging is extremely dependent on the seeing quality. It can be shown that optimizing according to the atmospheric conditions leads to a S/N dependence on the seeing angle W of the form $S/N \approx W^{-4 \text{ to } 5}$ The total integration time and the exposure time have a much smaller effect (see Table 2). This means that the source magnitude and the seeing alone almost completely drive the quality of the result or, conversely, that it is *unrealistic* to intend to compensate for poor observing conditions by much longer integration times. On the contrary, the accessible resolution must be derived from these conditions and the

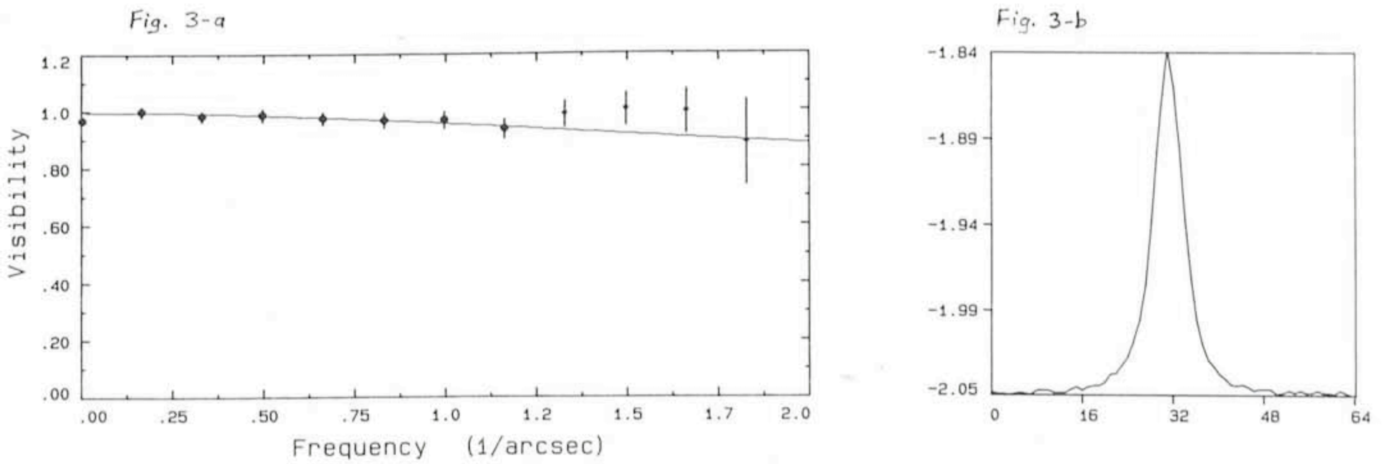

Figure 3: *(a) Visibility at K of a source of magnitude 8.9 observed with the 0.46 arcsec wide slit. Exposure time: 250 ms. 2,700 scans retained out of a 96-mn total observing time (reference included). The solid line is a binary model fit with a secondary fractional flux ratio of 6.5 % drawn for deriving the maximum separation consistent with these assumptions and data (0.20 arcsec).*
(b) Coadded recentred scans from the same set of data s in (a). Seeing at V: 1.3 arcsec; full scale: 6.0 arcsec. A source of a K magnitude 14.5 would be 3 times higher than the rms noise and would clearly show up if it were at more than 1 arcsec from the central source.

relevant parameters (slit width, exposure time, amplitude, temporal frequency range . . .) choosen accordingly and modified as those ones change. Here is certainly the difficult side of this technique!

Medium resolution imaging is much less affected by the seeing. The performances are derived by taking into account the system or sky limitations as in photometry. It can be seen (Table 2) that the sensitivity is of course lower than with a photometer but a resolution of 0.5 arcsec can here be routinely achieved. This mode can also be an excellent back-up in case of bad conditions.

Examples showing the result of two opposite optimizations are shown in Figure 2 and 3. The data were obtained under good conditions, yet for Figure 2 the number of scans was not large enough to reach the background limitation. In this case the uncertainty computed at each spatial frequency results essentially from the seeing statistics (note that the values in Table 2 assume a stationary seeing); as contiguous points are not independent, the visibility may present some oscillations which are not real. That is why such a visibility must be fitted by a model of at most 3 or 4 parameters.

Treatment

Some reduction is done in real time aiming to the estimation of the observation quality but the final results rely on a more sophisticated treatment applying algorithms of image selection according to the seeing. Figures 2 and 3 display data from March 1986 reduced in this way with the software available at ESO (at La Silla and Garching, on an HP computer) and show the standard outputs of it. For many sources, these will be sufficient to extract the useful information by means of simple fits. The reduction package includes a fitting module with a model of one to three components of variable size, fractional flux and location; their individual intensity distribution being choosen from a set of analytical functions or stored in the form of a discrete set of intensities.

More elaborate processes like co-added-images deconvolution or image restoration are not currently included in this package. The observer willing to apply his own method can either use the raw data stored on tape as blocs of scans or the files created by the reduction software containing processed data like sorted scans or calibrated power spectra.

Contributions

This specklegraph was designed and integrated under ESO contract at Observatoire de Lyon (sup. F. Sibille), INAG (M. Jegou) and Laboratoire IR de Meudon. The ESO infrared group contributed to the qualification and tests. The software was provided by C. Perrier with support from F. Gutierrez. Special thanks are due to T. Bohl, C. Marlot and J. Roucher who were deeply involved at the integration or testing stages.

The Fast-Photometry Facilities at La Silla

P. BOUCHET and F. GUTIERREZ, ESO, La Silla

We briefly present in this note the available programme (and its environment) to perform fast photometry at La Silla. This facility has become available on the mountain a long time ago already but recent discussions with some Visiting Astronomers tend to show that potential users are not yet well aware of it. Many programmes have already been carried out with this mode of observing, mainly in the infrared but also in the visible. Let us mention, for instance:

– Occultations of stars by planets to discover and/or study rings as well as to determinate the temperatures and variations of the atmospheres of the planets. (See for instance: Bouchet et al., *The Messenger* No. 26, Dec. 1981 and Haefner et al., *The Messenger* No. 42, Dec. 1985).

– The mutual phenomena of Jupiter, observed through the international PHEMU 85 campaign (Arlot et al., same issue of *The Messenger*).

– Search for flare or rapid variations in cataclysmic variables (Motch et al., *The Messenger* No. 26, Dec. 1981).

The "Time Series Photometry Programme" (TSPP) consists of a set of counters that are read each millisecond and can be used at any telescope equipped with a standard 21 MX computer extender, which are presently the ESO 3.6 m and 1.0 m, and the Danish 1.5 m. However, for special cases it could be possible to implement it at the ESO 50 cm too. Up to 4 counters are synchronized with a 1 Kilo-Hertz signal from a CERME clock display unit. This clock is connected to the ESO Universal Time. The computer is connected to the CERME to read out the UT. Every 10 seconds the synchronization of the computer internal time and the CERME time is checked. In case of a lost synchronization, the programme will reset it at the next 10th second change (in that case, 10 seconds of observations would have been lost). The CERME clock provides also a 1 kHz signal to read the counters each millisecond.

The user chooses the time resolution called TBASE. The acquisition is made by adding the counts read each millisecond from the scalers during the time TBASE and saving the sum in a floating point internal buffer. When this buffer is full, it is sent to the magtape unit. This procedure is made through two independent buffers. While one is saving data, the other one is dumping its data to the magtape, and reverse. In this way no data are lost during the external dump.

The computer is also connected to a Strip Chart recorder which enables the observer to see ON LINE the input data at a time resolution selected by him. The programme foresees the possibility to be connected to the ESO Standard photometers to provide control over the filters and diaphragm wheels and over the shutters.

Data obtained from the TSPP acquisition environment can be reduced at the HP-1000 system at the computer centre at La Silla. This is done using several programmes written by Ch. Motch which:

– list a catalogue of all the records present in a magtape file;

– read several consecutive records, plot any part of the data in memory, make a listing of the measurements, change them eventually, compute averages and dump data in a disk file;

– copy records in any file from magtape;

– perform a Fourrier transformation on a block of 2,048 measurements in the same channel;

– compute autocorrelation function on blocks of 2,048 measurements in the same channel.